Solid-State Phase-Change Heterostructures for Radiative Heating and Cooling in Space

Sam Keller[1, 2], Yujie Luo[2], Daniel Kindem[2], Karl Pederson[2], and Ognjen Ilic[3]
University of Minnesota – Twin Cities, Minneapolis, Minnesota, 55455

High-power satellites offer promising new imaging and communications capabilities, yet there exist significant thermal management challenges for satellites with a limited radiating surface area. Conventional approaches for mitigating overheating use deployable radiators to increase total heat rejection and louvers to switch between heating and cooling states. These components are often mechanical and can exhibit high broadband emissivity, such as for radiators comprising composite graphite coatings. As a result, these radiators can absorb unwanted solar irradiation, which reduces their cooling potential. We present an approach for radiative thermal management using few-layer optical heterostructures comprising solid-state phase-change materials that exhibit a tunable refractive index, enabling dynamic control of emissivity. The thickness and material composition of these layered structures may be optimized to switch between reflecting solar radiation and emitting long-wavelength radiation in a cooling state and absorbing solar radiation while reflecting long-wavelength radiation in a heating state. We describe the design and optimization procedure for these structures and show that radiators that incorporate phase-change materials could reach temperatures below a blackbody emitter through selective reflection of solar radiation. We initially evaluate thermochromic and electrochromic materials and then analyze the use of chalcogenide glasses as an active variable emissivity thermal management solution. In addition to having a highly reversible solid-state phase transition, chalcogenide glasses remove the need for mechanical actuation of louvers and thermal switches when alternating between heating and cooling. Furthermore, they require no net electrical power to maintain either state.

Acronyms and Nomenclature

α_h	=	hemispherical absorptivity
ε_h	=	hemispherical emissivity
θ	=	incidence angle
λ	=	wavelength
ϕ	=	azimuthal angle
c	=	speed of light
h	=	Planck's constant
I_b	=	blackbody radiance
k	=	Boltzmann's constant
N	=	number of layers
R_h	=	hemispherical reflectivity
T	=	temperature
t	=	thickness
FOM	=	figure of merit
LEO	=	Low Earth Orbit
PCM	=	phase-change material

[1] NSTGRO Fellow, Department of Mechanical Engineering, 111 Church Street SE, Minneapolis, MN 55455.
[2] Research Assistant, Department of Mechanical Engineering, 111 Church Street SE, Minneapolis, MN 55455.
[3] Assistant Professor, Department of Mechanical Engineering, 111 Church Street SE, Minneapolis, MN 55455.

I. Introduction

Thermal management in space remains a complex optimization of generated and dissipated heat. With state-of-the-art spacecraft aiming to explore harsh new environments, maintaining a stable temperature is critical to a successful mission. In addition to designing for new environments, thermal management solutions must also account for the heat generated and stored aboard these spacecraft. The inclusion of high-power imaging systems and precise electronics have been observed to constrain the functional operating temperature range of satellites. Heat dissipation must occur through conduction within the spacecraft body and radiation to space. Without properly engineering its radiating surfaces, heat can remain trapped due to low thermal emission. To address this bottleneck in heat transfer, we examine the use of phase-change materials as a variable emissivity coating. These materials display a reversible solid-state phase transition, resulting in contrasting optical properties between states. Using this principle, we aim to establish a single material capable of cooling through solar reflection and thermal emission and heating through solar absorption and thermal reflection, as seen in **Figure 1**. This concept is key for ensuring satellites remain at consistent temperatures when facing the Sun and when the Sun is eclipsed by Earth. Additionally, variable emissivity coatings present a novel thermal regulation solution for future habitats on the Moon and Mars.

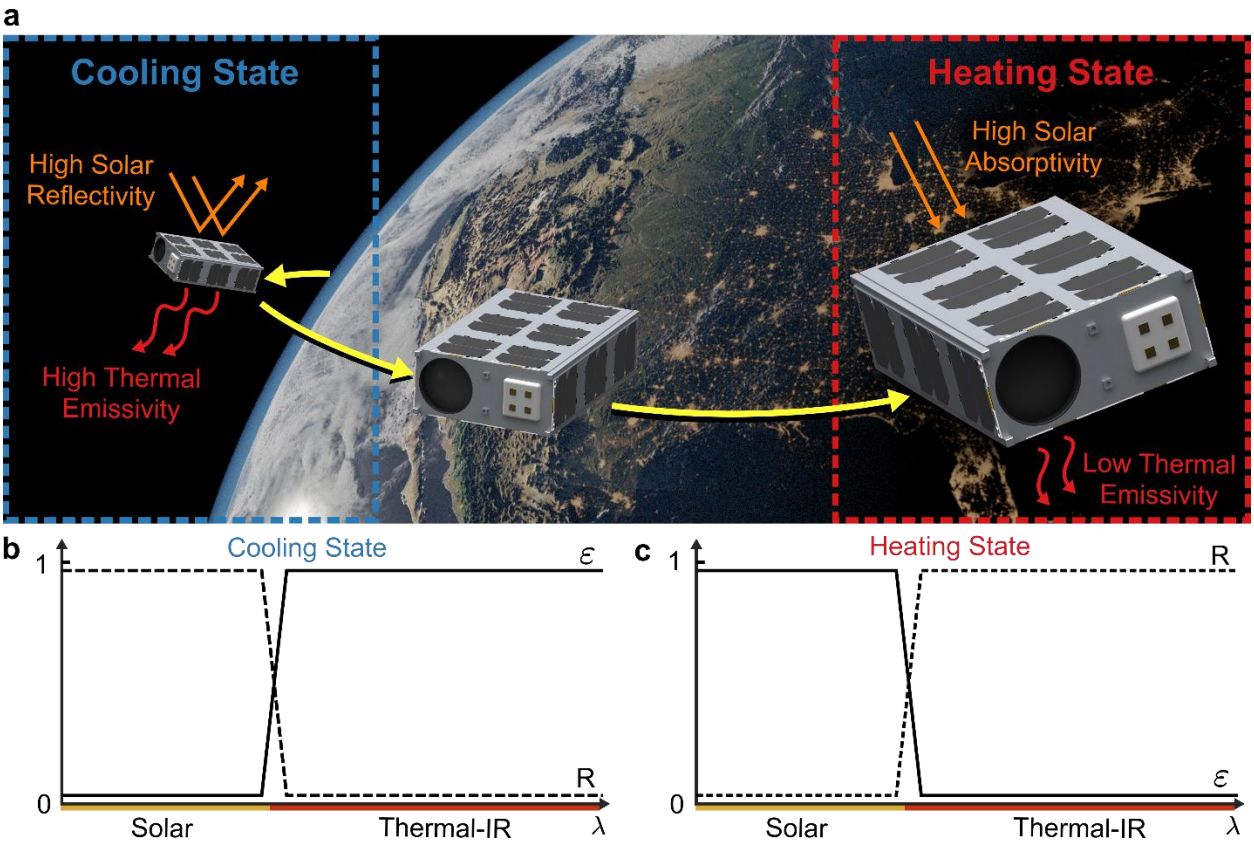

Figure 1. (a) Variable emissivity heating and cooling concept. (b) Cooling state with low solar absorptivity and high thermal emissivity. (c) Heating state with high solar absorptivity and low thermal emissivity.

In this work, we discuss the materials selection and optimization of few-layered variable emissivity devices using a residual neural network to efficiently explore the non-convex design space. The method presented is able to account for lossy materials and can easily be adapted to a wide variety of phase-change materials with known optical properties. We first establish a figure of merit for heating and cooling in space and then use this to optimize various few-layer emitters comprising both thermochromic materials and chalcogenide glasses as the phase-change material. The tradeoff between structure complexity and emissivity contrast will then be evaluated and avenues for future work will be proposed.

A. Phase-Change Materials as Variable Emissivity Devices

Thermochromic materials are a passive variable emissivity solution to thermal management in space. These materials exhibit a temperature-driven reversible phase transition between metallic and insulating states. For many such materials, these states display highly contrasting refractive indices over solar and infrared wavelengths, making them an ideal candidate for thermal management in space. In particular, vanadium dioxide (VO_2) and lanthanum strontium manganite (LSMO) have been extensively studied for this environment due to their phase transition temperature lying within the standard operation range of most spacecraft and satellites.[1,2] This results in a single material which passively switches between heating and cooling states to achieve a temperature near that of the phase change. Despite not requiring any power to change state, the functionality of these materials often relies on precisely engineering the phase transition temperature to lie within the operating range for a given spacecraft. For state-of-the-art small spacecraft and CubeSats, the maximum allowable temperature for most electronics ranges from 50-60°C,[3,4] while bulk VO_2 exhibits a metal-insulator phase-change at a temperature of 68°C.[5,6] The onset temperature for this phase transition can be reduced through the process of doping with materials such as tungsten; however, this has been found to significantly decrease the infrared optical contrast between phases.[7,8]

Electrochromic materials, unlike their thermochromic counterpart, do not rely on a constant temperature to maintain state. The phase-change of these materials is induced by applying a relatively low voltage (~1V).[10] Once this transition occurs, electrochromic materials are able to retain their state for extended periods of time without any applied voltage due to their optical memory.[11] As a result, these materials have been largely studied as active thermal management solutions. The benefit of these materials is their lack of reliance on temperature to induce phase-change, allowing them to be designed and optimized independently of the specific thermal requirements of a spacecraft. Metal oxides such as tungsten trioxide (WO_3) have demonstrated emissivity modulation over near-IR wavelengths.[12,13] Recent studies have identified layered conductive polymers as a potential electrochromic variable emissivity device;[14–16] however, it remains unclear if these devices are capable of withstanding the radiation, pressure, and temperatures associated with a typical space environment.

Chalcogenide glasses display a reversible and continuous transition between amorphous and crystalline phases when annealed above a specified temperature. This phase change is commonly onset via joule heating for large, uniform films or focused laser irradiation for high spatial resolution in applications such as optical storage devices, IR sensors, and optical circuits.[17,18] Of these materials, germanium antimony tellurium (GST-225), a well-studied solid-state phase-change material, exhibits ultrafast transitions: amorphous to face-centered cubic (~150°C), then to hexagonal close-packed (~360°C), and back to amorphous (~580°C), all within microseconds.[19] It has been demonstrated that the phase-change of these materials may remain stable over a long period without any applied voltage or temperature.[20] Additionally, they boast high tolerance to the repeated thermal cycling necessary to keep a spacecraft at operational temperature over the course of an orbit. Due to the rapid solid-state phase change of chalcogenide glasses, a pulsed applied voltage may be used to switch optical states, reducing their power consumption when compared to electrochromic devices which required a constant voltage supply. While constant power is not required to maintain state, these materials do exhibit an amorphous-crystalline temperature well above the limits for most spacecraft. Even greater is the crystalline-amorphous phase transition temperature. Rapid thermal cycling of these materials on a large scale poses a significant challenge which has yet to be addressed. Despite this, recent studies aboard the MISSE-14 platform located on the International Space Station (ISS) have revealed the durability of GST-225 in Low Earth Orbit (LEO).[21]

B. Emitter Design and Optimization Procedure

The design and optimization of multi-layered optical heterostructures remains a consistent challenge due to its non-convex nature. Arriving at a globally optimal structure requires this design space to be fully explored. Previous studies have explored this problem through the use of genetic algorithms;[22,23] however, this approach is gradient-free resulting in a higher likelihood of solving for a local optima. Recently, the use of generative neural networks has been identified as an effective way to optimize optical devices.[24] These neural networks are initially used to generate a set of layered materials for which the optical properties are calculated and a loss function is propagated back into the neural network to train subsequent material sets. This approach, as seen in **Figure 2**, has been modified for the specific design of two-phase selective emitters, which account for lossy materials. Initially, a uniformly distributed random noise vector is generated and used as an input for the residual neural network generator. This produces a distribution of multi-layered materials, which can have variable thicknesses and refractive indices. This procedure assumes each layer can be a combination of multiple materials, and as such, the refractive index produced by the neural network does not represent

a real material but rather a combination of all materials included. These complex layers are then simplified using a probability matrix to determine the contribution of materials in each layer. Using this information, the layer is then binarized according to the probability matrix and a single material and thickness is selected. This process is repeated for both optical states of the phase-change material. The layer composition, including thickness and complex refractive index, is then used to solve for the total reflectivity and emissivity of the material using the impedance method. The emissivity of both states is then weighted using solar and thermal blackbody radiation to determine average solar absorptivity and thermal emissivity. Updating and training the neural network relies on backpropagating the gradient of our Figure of Merit (FOM). Conventional radiators aim to minimize the solar absorptivity and maximize thermal emissivity; however, these devices are intended for single state cooling. Using solid-state phase-change materials, we aim to create a single device capable of heating through high solar absorption and low thermal emission, and cooling via low solar absorption and high thermal emission. Thus for a two-phase material intended for heating and cooling, we aim to maximize the contrast in solar absorption, α from 0.3-4.0μm, and thermal emission, ε from 4.0-20.0μm for two unique phases. For a single material with binary optical states, this becomes:

$$FOM = \left|\alpha_{h,a} - \alpha_{h,b}\right| + \left|\varepsilon_{h,b} - \varepsilon_{h,a}\right| \tag{1}$$

where a and b represent two optical states of variable thermal emissivity and solar absorptivity materials. For and material capable of perfect solar heating and radiative cooling in different optical states our FOM approach a value of 2, indicating the maximum possible solar absorptivity and thermal emissivity contrast. We evaluate hemispherically averaged absorptivity and emissivity to ensure consistent performance regardless of orientation with respect to the Sun. The gradient of this metric was then used to update the neural network training over each iteration as seen in **Figure 2**.

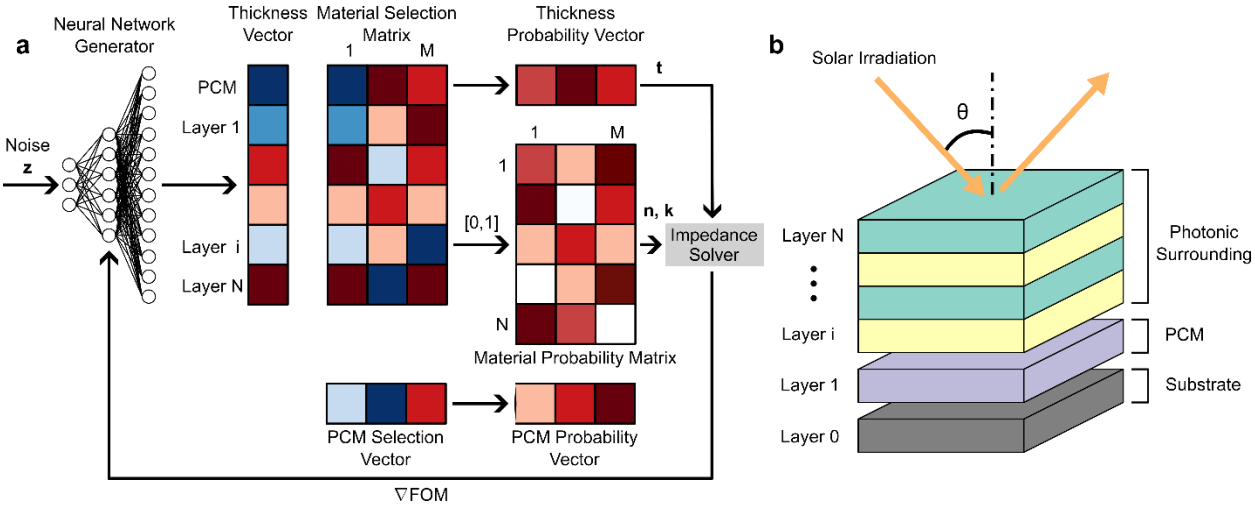

Figure 2. (a) Multi-layer residual neural network optimization procedure including single-layer phase-change materials. (b) Output heterostructure optimized over a range of solar incidence angles.

Several specifications are initially made using this approach. First, we set the substrate material to be aluminum with sufficient thickness to prevent transmission over the wavelength range in question. This assumption allows for our layered materials to be deposited directly on existing satellite busses and radiator structures but does not account for a joule heating element being placed in contact with the chalcogenide glass layer. We then specify that the phase-change material must be located directly above the substrate, or the first layer of the heterostructure. This assumption is critical to designing a device which can not only be fabricated, but also reversibly switched between states. For thermochromic materials, direct contact with a conductive substrate ensures a rapid response to overall spacecraft temperature in a dynamic environment. This requirement is also beneficial for chalcogenide glasses and electrochromic materials, which require a conductive electrode or resistive heater to achieve phase transition. Lastly, the neural network approach requires that we specify a wavelength range, total number of layers, and maximum thickness for each layer.

II. Results

The residual neural network described above was first used to optimize single-layer phase-change emitters. These devices comprise a phase-change material placed directly above a thick aluminum substrate. The complex refractive index of both material phases is then used to solve for the emissivity of both states simultaneously. This process was initially performed assuming vanadium dioxide (VO_2) to be the phase-change material, resulting in an optimal thickness of 225 nm for this configuration. The two phases for VO_2 are based on the optical properties at 25°C and 100°C.[25] We note that single-layer VO_2 emitters display poor cooling capabilities resulting from high solar absorptivity in both states. A library of various chalcogenide glasses was then established and incorporated into the optimization workflow to include both material and thickness analysis. A list of all phase-change materials studied can be found in the appendix. The resulting hemispherical emissivity for these single-layer materials is found in **Figure 3**. The single layer vanadium dioxide emitter has a average solar absorptivity of 0.62 and thermal emissivity of 0.096 at 25°C and solar absorptivity of 0.58 and thermal emissivity of 0.29 when heated to 100°C. The single layer chalcogenide glass emitter has a average solar absorptivity of 0.39 and thermal emissivity of 0.08 when amorphous and solar absorptivity of 0.39 and thermal emissivity of 0.43 when annealed to the crystalline state. We see an improvement in the FOM of >0.24 when considering chalcogenide glasses over vanadium dioxide for the phase-change material. In particular, germanium-antimony-selenium-tellurium (GSST) provides the greatest absorptivity and emissivity contrast, with an FOM of 0.49. In its crystalline cooling state, GSS_2T_3 displays significantly lower solar absorptivity when compared to previous thermochromic materials.

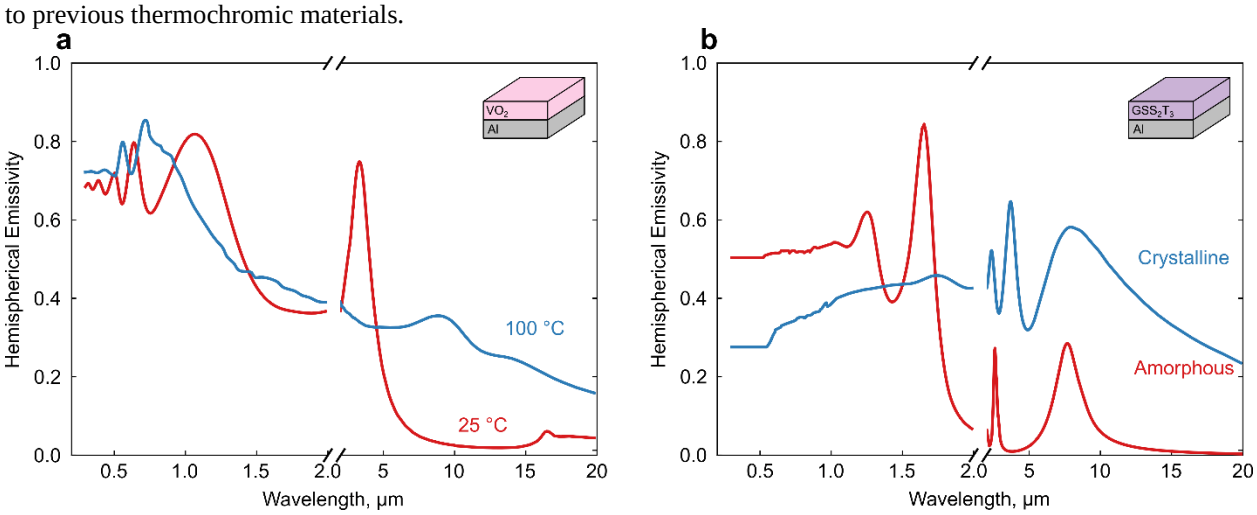

Figure 3. (a) Single-layer optimization of a VO_2 emitter. (b) Single-layer optimization of a chalcogenide glass emitter.

To improve the emissivity contrast between states and increase our figure of merit, we reoptimize both thermochromic and chalcogenide glass based heterostructures to include few-layered photonic surroundings. The complete material library used for this structure can be found in the Appendix. It comprises various materials used in thin film optics over UV and IR wavelength ranges. We observe that alternating layers of germanium, zinc selenide, and barium fluoride provide the greatest optical contrast between states. We present the hemispherical emissivity for few-layered thermochromic and chalcogenide glass emitters below. These examples highlight the performance improvement of increasing the total number of layers included in the optimization. A vanadium dioxide emitter with two layer photonic surrounding has a average solar absorptivity of 0.62 and thermal emissivity of 0.15 at 25°C and solar absorptivity of 0.65 and thermal emissivity of 0.68 when heated to 100°C. The chalcogenide glass, now GSS_3T_2, emitter with two layer photonic surrounding has a average solar absorptivity of 0.49 and thermal emissivity of 0.076 when amorphous and solar absorptivity of 0.69 and thermal emissivity of 0.80 when annealed to the crystalline state. When we optimize a vanadium dioxide emitter with four layer photonic surrounding we see an average solar absorptivity of 0.49 and thermal emissivity of 0.15 at 25°C and solar absorptivity of 0.51 and thermal emissivity of 0.67 when heated to 100°C. The chalcogenide glass emitter with four layer photonic surrounding has a average solar absorptivity of 0.52 and thermal emissivity of 0.087 when amorphous and solar absorptivity of 0.74 and thermal emissivity of 0.89 when annealed to the crystalline state. As seen in **Figure 4**, the FOM for a VO_2 few-layer emitter increases to 0.67 when our optimization increases to five layers. Similarly, the FOM for a GSS_3T_2 few-layer emitter increases to 0.92. Of particular interest is the identical material selection for both phase-change materials. The thicknesses associated with

each layer can be found in the Appendix. In general, we see a decrease in the solar absorption contrast but an increase in thermal-IR contrast when increasing the number of surrounding photonic layers.

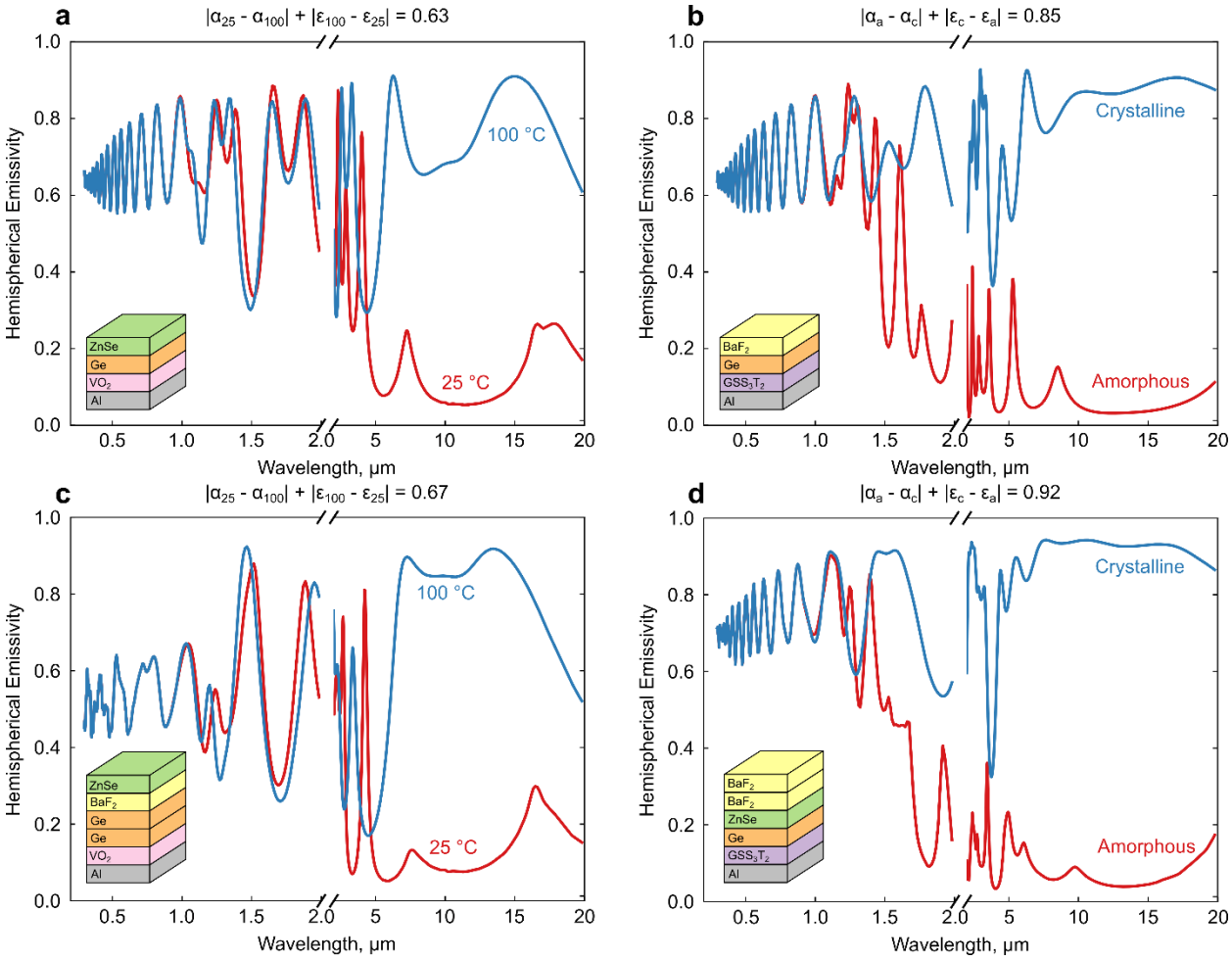

Figure 4. (a) Three-layer optimization of a VO_2 emitter. (b) Three-layer optimization of a chalcogenide glass emitter. (c) Five-layer optimization of a VO_2 emitter. (d) Five-layer optimization of a chalcogenide glass emitter.

We observe that the figure of merit previously described is indeed providing suitable thermal emissivity contrast; however, the introduction of increasingly thick photonic surroundings not only decreases the solar absorption contrast, but increases the total solar absorption as well. For the case of the chalcogenide glass based emitters, we can clearly see that a heating state (high absorptivity, low emissivity) is reached, yet the cooling state (low absorptivity, high emissivity) is less clear. Our complex materials display relatively high broadband emissivity which will result in the absorption of unwanted solar irradiation in this state. Possible methods to reduce the absorption in this state will be discussed later, though a redefinition of the figure of merit may also produce more suitable materials which display low solar absorptivity in both states.

Lastly, we present the tradeoff between emissivity contrast and number of layers for thermochromic and chalcogenide glass heterostructures designed using the neural network approach. As seen in **Figure 5**, we observe diminishing performance enhancement with increasing number of layers. For the various structures designed in this study, it was determined that a three-layer stack for both thermochromic and chalcogenide glass based emitters provides a suitable tradeoff between material complexity and emissivity/absorptivity contrast.

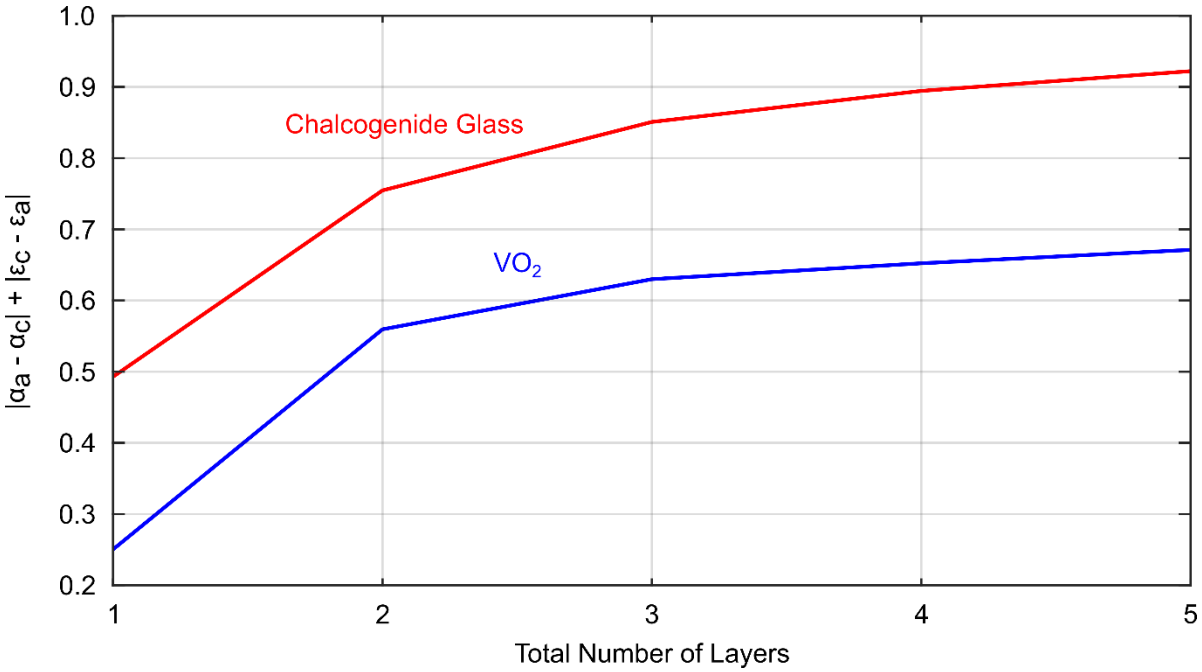

Figure 5. Figure of merit for various numbers of emitter layers using thermochromic and chalcogenide phase-change materials.

III. Methods

We assume the temperature of the Sun to be $T_{sol} = 5777K$ and the temperature of our radiator to be $T_{th} = 300K$. This temperature was selected to lie within the standard operating range of most components contained within small spacecraft; however, the actual radiator temperature is dependent on the power consumption of specific internal components. Using these values, the blackbody spectral radiance is given by:

$$I_b(\lambda, T) = \frac{2\pi hc}{\lambda^5(e^{\frac{hc}{\lambda kT}} - 1)} \tag{2}$$

A library is then established to include various phase-change and photonic surrounding materials. Using the previously described residual neural network, a thickness vector, material selection matrix, and PCM selection vector are generated. The values in these matrices are initially unbounded to provide a more stable optimization and convergence of the loss function. This means the material selection matrix and PCM selection vector do not assume a categorical constraint on the refractive index. Instead, it is assumed that each layer is made up of a complex combination of all materials. The values within each matrix and vector are then restricted to lie between zero and one through the use of sigmoid and softmax functions. This establishes a probability matrix which reinforces categorical constraints on the refractive index of each layer, ensuring the output structure contains real materials and thicknesses for each layer. The resulting thickness and complex refractive index for each layer is used as input for an impedance solver to identify the unpolarized reflection by averaging both s- and p- polarized light at various angles of incidence. The unpolarized hemispherical reflection for a given wavelength and material state is then determined using the following relation:

$$R_h = \frac{\int_0^{2\pi}\int_0^{\pi/2} R(\theta,\phi)\cos\theta\sin\theta \mathrm{d}\theta\mathrm{d}\phi}{\int_0^{2\pi}\int_0^{\pi/2} \cos\theta\sin\theta \mathrm{d}\theta\mathrm{d}\phi} \tag{4}$$

Where R is the reflectivity, θ is the incidence angle, and ϕ is the azimuthal angle. By affixing an optically thick aluminum layer to the bottom of our emitter, we can assume zero transmission over UV and IR wavelengths, allowing us to determine the hemispherical emissivity at a given wavelength for both states using the following formula:

$$\alpha_h = \varepsilon_h = 1 - R_h \tag{5}$$

Finally, we can determine the solar absorptivity and thermal emissivity by weighting the total hemispherical emissivity with blackbody spectral radiance at our assumed solar and thermal temperatures using the following equations:

$$\alpha_{h,sol}(T) = \frac{\int \alpha_{sol}(\lambda) I_b(\lambda, T_{sol}) \mathrm{d}\lambda}{\int I_b(\lambda, T_{sol}) \mathrm{d}\lambda} \tag{6}$$

$$\varepsilon_{h,th}(T) = \frac{\int \varepsilon_{th}(\lambda) I_b(\lambda, T_{th}) \mathrm{d}\lambda}{\int I_b(\lambda, T_{th}) \mathrm{d}\lambda} \tag{7}$$

When optimizing few-layered heterostructures using the neural network approach described, an upper bound must be set to the layer thickness. This was limited to $1.0\ \mu m$ after observing that a lower limit results in several layers of the same material being placed together in the optimized material. Increasing the layer thickness limit allows us to better explore the effects of alternating material layers in addition to material thickness. Additionally, the wavelength limits were set from $0.3 – 20.0\ \mu m$ due to the limited range of available refractive index data for various materials. Beyond the wavelength range studied here there exists non-zero thermal emission which should be accounted for. The decreasing emissivity contrast of our optimized GSS_3T_2 emitters near 20μm indicates the inclusion of longer wavelengths may decrease our figure of merit.

IV. Summary and Conclusion

We adopted a neural network-based design approach to optimize variable emissivity coatings for spacecraft heating and cooling. This approach is successful at identifying few-layer structures capable of significant radiative thermal contrast. This optimization procedure was used to design emitters comprising both thermochromic and chalcogenide glasses as the phase-change material. For a chalcogenide glass emitter with four layer photonic surrounding we achieve a thermal emissivity contrast of 0.81 between states using this approach. A similarly designed structure with a vanadium dioxide emitter only reaches a thermal emissivity contrast of 0.52. While these materials may have different applications due to mechanisms associated with their respective phase transitions, we show that for single-layer and few-layer structures, GSS_2T_3 results in a greater figure of merit than VO_2, one of the most commonly studied thermochromic materials for space. We then discuss the tradeoff between the number of material layers and our figure of merit to highlight the diminishing return on optical performance when thickness is increased. Evaluating this from a fabrication cost and total mass perspective will give a true understanding of the ideal number of layers for any given variable emissivity device.

The procedure used here may be directly applied to the study of any variable emissivity device which exhibits binary states. The assumption that our phase-change material may only reach two distinct states is made to simplify computation and allow for design using preexisting refractive index data for the various materials selected. For both thermochromic materials and chalcogenide glasses, the phase transition is continuous, allowing for intermediate states to be reached. Experimental evaluation of the optical characteristics of these intermediate states may result in increased emissivity contrast. Additionally, these intermediate states could be used to more precisely tune the heating and cooling limits of the structure in an effort to maintain a more stable temperature. Future work will aim to fabricate few-layer solid-state phase-change materials and characterize their optical and thermal performance in a near-space environment. We then expect to incorporate the continous phase transition of chalcogenide glasses into emitter optimization to better understand the thermal control and switching of these devices.

Lastly, we note the high solar absorption associated with the various materials designed in this work. While our figure of merit aims to produce high absorptivity and emissivity contrast, there exists a tradeoff between these two. Increasing layer thickness and total number of layers reduces the solar contrast and increases the thermal contrast between states. Additionally, the optically thick materials produced show high solar absorption, a poor characteristic for reaching a cooling state. Future work will aim to reduce solar absorption in both states through inclusion of new materials and surface patterning. Nonetheless, the presented design approach is general and can be adapted to optimize for different heating and cooling balances by redefining the optimization loss function or incorporating new materials and thickness limitations.

Appendix

Table 1. List of materials included in the photonic surrounding and phase-change layer.

Photonic Surrounding Materials	Phase-Change Materials
SiO2	GST-225
Al2O3	GSS2T3
HfO2	GSS3T2
TiO2	GSS1T4
ZrO2	GSS4T1
MgF2	GSS
BaF2	Sb2Se3
a-Si	Sb2S3
ZnSe	VO2
Ge	
ZnS	
Si3N4	

Table 2. List of materials and thicknesses for thermochromic emitters of 1, 3, and 5 layers.

1-Layer Emitter		3-Layer Emitter		5-Layer Emitter	
Material	Thickness, μm	Material	Thickness, μm	Material	Thickness, μm
VO_2	0.255	VO_2	0.318	VO_2	0.311
		Ge	0.460	Ge	0.268
		ZnSe	0.934	Ge	0.268
				BaF_2	0.770
				ZnSe	0.319

Table 3. List of materials and thicknesses for chalcogenide glass emitters of 1, 3, and 5 layers.

1-Layer Emitter		3-Layer Emitter		5-Layer Emitter	
Material	Thickness, μm	Material	Thickness, μm	Material	Thickness, μm
GSS_2T_3	0.423	GSS_3T_2	0.633	GSS_3T_2	0.632
		Ge	0.431	Ge	0.416
		ZnSe	0.948	ZnSe	0.827
				BaF_2	0.753
				BaF_2	0.727

Acknowledgments

SK acknowledges support through the NASA Space Technology Graduate Research Opportunities (NSTGRO) fellowship 80NSSC24K1372. The authors acknowledge support by DARPA (award number D24AP00310-00) and the Office of Naval Research (award number N00014-23-1-2627). We thank J. Hu for the helpful discussion.

References

1 Shiota, T., Sato, K., Cross, J. S., Wakiya, N., Tachikawa, S., Ohnishi, A., Sakurai, O., and Shinozaki, K., "Thermal Radiative Properties of (La1−xSrx)MnO3−δ Thin Films Fabricated on Yttria-Stabilized Zirconia Single-Crystal Substrate by Pulsed Laser Deposition," *Thin solid films*, Vol. 593, 2015, pp. 1–4.

2 Taylor, S., Yang, Y., and Wang, L., "Vanadium Dioxide Based Fabry-Perot Emitter for Dynamic Radiative Cooling Applications," *Journal of quantitative spectroscopy & radiative transfer*, Vol. 197, 2017, pp. 76–83.

3 Yost, B., Weston, S., Benavides, G., Krage, F., and Hines, J., "State-of-the-Art Small Spacecraft Technology," 2021. https://ntrs.nasa.gov/api/citations/20210021263/downloads/2021_SOA_final_508_updated.pdf

4 Diaz-Aguado, M. F., Greenbaum, J., Fowler, W. T., and Glenn Lightsey, E., "Small Satellite Thermal Design, Test, and Analysis," In *Modeling, Simulation, and Verification of Space-based Systems III*, Vol. 6221, 2006, pp. 74–85.

5 Barker, A. S., Verleur, H. W., and Guggenheim, H. J., "Infrared Optical Properties of Vanadium Dioxide above and below the Transition Temperature," *Physical review letters*, Vol. 17, No. 26, 1966, pp. 1286–1289.

6 Voti, R. L., Larciprete, M. C., Leahu, G., Sibilia, C., and Bertolotti, M., "Optimization of Thermochromic VO2 Based Structures with Tunable Thermal Emissivity," *Journal of applied physics*, Vol. 112, No. 3, 2012, p. 034305.

7 Liu, D., Cheng, H., Xing, X., Zhang, C., and Zheng, W., "Thermochromic Properties of W-Doped VO 2 Thin Films Deposited by Aqueous Sol-Gel Method for Adaptive Infrared Stealth Application," *Infrared physics & technology*, Vol. 77, 2016, pp. 339–343.

8 Victor, J. L., Marcel, C., Sauques, L., Labrugère, C., Amiard, F., Gibaud, A., and Rougier, A., "From Multilayers to V1-XWxO2±δ Films Elaborated by Magnetron Sputtering for Decreasing Thermochromic Transition Temperature," *Journal of alloys and compounds*, Vol. 858, No. 157658, 2021, p. 157658.

9 Youngquist, R. C., Nurge, M. A., Johnson, W. L., Gibson, T. L., and Surma, J. M., "Cryogenic Deep Space Thermal Control Coating," *Journal of spacecraft and rockets*, Vol. 55, No. 3, 2018, pp. 622–631.

10 Demiryont, H., and Shannon, K., "Variable Emittance Electrochromic Devices for Satellite Thermal Control," *AIP conference proceedings*, Vol. 880, 2007, pp. 51–58.

11 Somani, P. R., and Radhakrishnan, S., "Electrochromic Materials and Devices: Present and Future," *Materials chemistry and physics*, Vol. 77, No. 1, 2003, pp. 117–133.

12 Hale, J. S., and Woollam, J. A., "Prospects for IR Emissivity Control Using Electrochromic Structures," *Thin solid films*, Vol. 339, Nos. 1–2, 1999, pp. 174–180.

13 Huang, Y.-S., Zhang, Y.-Z., Zeng, X.-T., and Hu, X.-F., "Study on Raman Spectra of Electrochromic C-WO3 Films and Their Infrared Emittance Modulation Characteristics," *Applied surface science*, Vol. 202, Nos. 1–2, 2002, pp. 104–109.

14 Chandrasekhar, P., Zay, B. J., Lawrence, D., Caldwell, E., Sheth, R., Stephan, R., and Cornwell, J., "Variable-emittance Infrared Electrochromic Skins Combining Unique Conducting Polymers, Ionic Liquid Electrolytes, Microporous Polymer Membranes, and Semiconductor/Polymer Coatings, for Spacecraft Thermal Control," *Journal of applied polymer science*, Vol. 131, No. 19, 2014.

15 Chandrasekhar, P., Zay, B. J., Birur, G. C., Rawal, S., Pierson, E. A., Kauder, L., and Swanson, T., "Large, Switchable Electrochromism in the Visible through Far-Infrared in Conducting Polymer Devices," *Advanced functional materials*, Vol. 12, No. 2, 2002, pp. 95–103.

16 Petroffe, G., Beouch, L., Cantin, S., Chevrot, C., Aubert, P.-H., Dudon, J.-P., and Vidal, F., "Thermal Regulation of Satellites Using Adaptive Polymeric Materials," *Solar Energy Materials & Solar Cells*, Vol. 200, 2019, p. 110035.

17 Ta'eed, V., Baker, N., Fu, L., Finsterbusch, K., Lamont, M., Moss, D., Nguyen, H. C., Eggleton, B., Choi, D., Madden, S., and Luther-Davies, B., "Ultrafast All-Optical Chalcogenide Glass Photonic Circuits," *Conference on Lasers and Electro-Optics*, 2007, pp. 1–2.

18 Kolobov, A. V., and Tominaga, J., "Chalcogenide Glasses in Optical Recording: Recent Progress," *Journal of Optoelectronics and Advanced Materials*, 2002.

19 Cil, K., Dirisaglik, F., Adnane, L., Wennberg, M., King, A., Faraclas, A., Akbulut, M. B., Zhu, Y., Lam, C., Gokirmak, A., and Silva, H., "Electrical Resistivity of Liquid Ge2Sb2Te5 Based on Thin-Film and Nanoscale Device Measurements," *IEEE transactions on electron devices*, Vol. 60, No. 1, 2013, pp. 433–437.

20 Mishra, S., Chaudhary, P., Yadav, B. C., Umar, A., Lohia, P., and Dwivedi, D. K., "Fabrication and Characterization of an Ultrasensitive Humidity Sensor Based on Chalcogenide Glassy Alloy Thin Films," *Engineered Science*, Vol. 15, No. 19, 2021, pp. 138–147.

21 Kim, H. J., Julian, M., Williams, C., Bombara, D., Hu, J., Gu, T., Aryana, K., Sauti, G., and Humphreys, W., "Versatile Spaceborne Photonics with Chalcogenide Phase-Change Materials," *NPJ microgravity*, Vol. 10, No. 1, 2024, p. 20.

22 Cuco, A. P. C., de Sousa, F. L., Vlassov, V. V., and da Silva Neto, A. J., "Multi-Objective Design Optimization of a New Space Radiator," *Optimization and Engineering. International Multidisciplinary Journal to Promote Optimization Theory & Applications in Engineering Sciences*, Vol. 12, No. 3, 2011, pp. 393–406.

23 Long, L., Taylor, S., Ying, X., and Wang, L., "Thermally-Switchable Spectrally-Selective Infrared Metamaterial Absorber/Emitter by Tuning Magnetic Polariton with a Phase-Change VO2 Layer," *Materials Today Energy*, Vol. 13, 2019, pp. 214–220.

24 Jiang, J., and Fan, J. A., "Multiobjective and Categorical Global Optimization of Photonic Structures Based on ResNet Generative Neural Networks," *Nanophotonics*, Vol. 10, No. 1, 2020, pp. 361–369.

25 Beaini, R., Baloukas, B., Loquai, S., Klemberg-Sapieha, J. E., and Martinu, L., "Thermochromic VO2-Based Smart Radiator Devices with Ultralow Refractive Index Cavities for Increased Performance," *Solar energy materials and solar cells: an international journal devoted to photovoltaic, photothermal, and photochemical solar energy conversion*, Vol. 205, No. 110260, 2020, p. 110260.